Diffusional Transformations in Solids

The majority of phase transformations that occur in the solid state take place by thermally activated atomic movements. The transformations that will be dealt with in this chapter are those that are induced by a change of temperature of an alloy that has a fixed bulk composition. Usually we will be concerned with the transformations caused by a temperature change from a single-phase region of a (binary) phase diagram to a region where one or more other phases are stable. The different types of phase transformations that are possible can be roughly divided into the following groups:

(a) precipitation reactions, (b) eutectoid transformations, (c) ordering reactions, (d) massive transformations, and (e) polymorphic changes. Figure shows several different types of binary phase diagrams that are representative of these transformations.

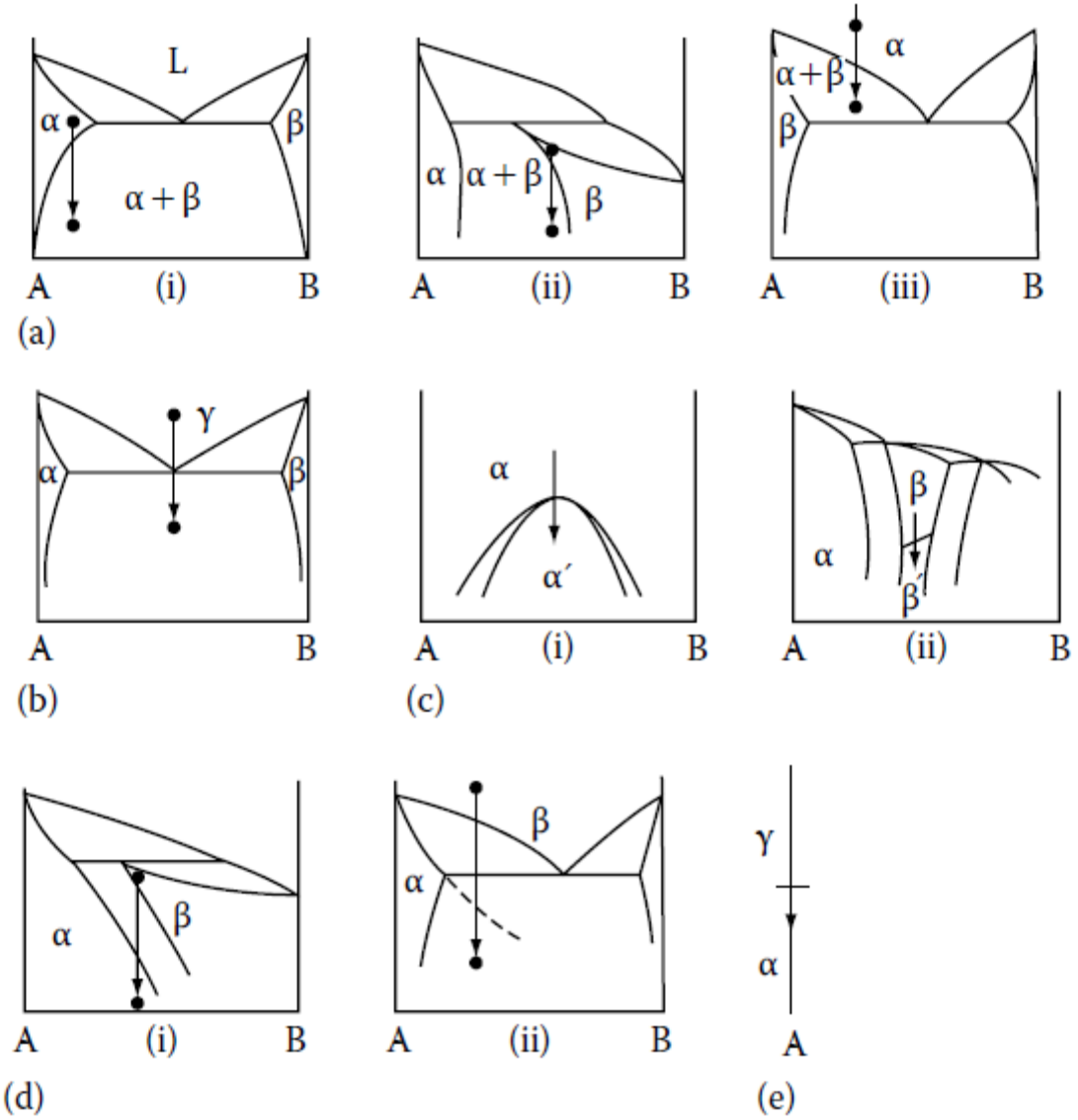

Examples of different categories of diffusional phase transformations: (a) precipitation; (b) eutectoid; (c) ordering; (d) massive; (e) polymorphic (single component).

Precipitation transformations can be expressed in reaction terms as follows:

$$\alpha' \rightarrow \alpha + \beta$$

where α' is a metastable *supersaturated solid solution*, β is a stable or metastable precipitate, and α is a more stable solid solution with the same crystal structure as α', but with a composition closer to equilibrium, see Fig-a.

Eutectoid transformations involve the replacement of a metastable phase (γ)

by a more stable mixture of two other phases ($\alpha + \beta$) and can be expressed as

$$\gamma \rightarrow \alpha + \beta$$

This reaction is characteristic of phase diagrams such as that shown in Fig-b.

Both precipitation and eutectoid transformations involve the formation of phases with a different composition to the matrix and therefore long-range diffusion is required.

The remaining reaction types can, however, proceed without any composition change or long-range diffusion. Fig-c shows phase diagrams where *ordering reactions* can occur. In this case the reaction can be simply written

$$\alpha(\text{disordered}) \rightarrow \alpha' \text{ (ordered)}$$

In a *massive* transformation the original phase decomposes into one or more new phases which have the same composition as the parent phase, but different crystal structures. Fig-d illustrates two simple examples of the type

$$\beta \rightarrow \alpha$$

where only one new phase results. Note that the new β phase can either be stable (Fig-d(i)) or metastable (Fig-d(ii)). *Polymorphic* transformations occur in single component systems when different crystal structures are stable over different temperature ranges, Fig-e. The most well-known of these in metallurgy are the transformations between fcc and bcc-Fe.

Apart from a few exceptions the above transformations all take place by diffusional nucleation and growth. As with solidification, nucleation is usually heterogeneous, but for the sake of simplicity let us begin by considering homogeneous nucleation.

Homogeneous Nucleation in Solids

To take a specific example consider the precipitation of B-rich β from a supersaturated A-rich α solid solution as shown in Fig-a(i). For the nucleation of β, B-atoms within the α matrix must first diffuse together to form a small volume with the β composition, and then, if necessary, the atoms must rearrange into the β crystal structure. As with the liquid → solid transformation an α/β interface must be created during the process and this leads to an activation energy barrier. The free energy change associated with the nucleation process will have the following three contributions.

1. At temperatures where the β phase is stable, the creation of a volume V of β will cause a volume free energy *reduction* of $V\,\Delta G_V$.

2. Assuming for the moment that the α/β interfacial energy is isotropic the creation of an area A of interface will give a free energy *increase* of $A\gamma$.

3. In general the transformed volume will not fit perfectly into the space originally occupied by the matrix and this gives rise to a misfit strain energy ΔG_s per unit volume of β. (It was shown in previous Chapter that, for both coherent and incoherent inclusions, ΔG_S is proportional to the volume of the inclusion.)

Summing all of these gives the total free energy change as

$$\Delta G = -V\Delta G_V + A\gamma + V\Delta G_s$$

If we ignore the variation of γ with interface orientation and assume the nucleus is spherical with a radius of curvature r, Equation becomes

$$\Delta G = -\frac{4}{3}\pi r^3(\Delta G_v - \Delta G_s) + 4\pi r^2\gamma$$

This is shown as a function of r in Fig. Note that the effect of the misfit strain energy is to reduce the effective driving force for the transformation to $(\Delta G_v - \Delta G_s)$. Similar curves would in fact be obtained for any nucleus shape as a function of its size.

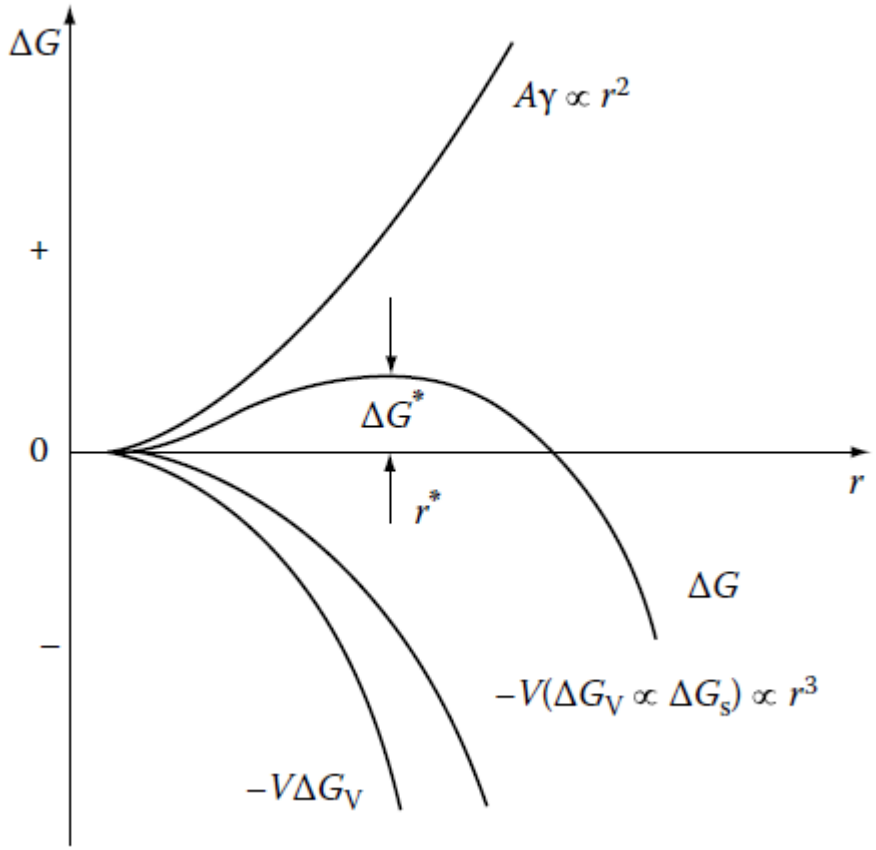

Differentiation of previous Equation yields

$$r^* = \frac{2\gamma}{(\Delta G_v - \Delta G_s)}$$

$$\Delta G^* = \frac{16\pi\gamma^3}{3(\Delta G_v - \Delta G_s)^2}$$

which is very similar to the expressions for solidification, except now the chemical driving force ΔG_v is reduced by a positive strain energy term. As discussed in previous Chapter, the concentration of critical-sized nuclei C^* will be given by

$$C^* = C_0 \exp(-\Delta G^*/kT)$$

where $C0$ is the number of atoms per unit volume in the phase. If each nucleus can be made supercritical at a rate of f per second the homogeneous nucleation rate will be given by

$$N_{\text{hom}} = f C^*$$

f depends on how frequently a critical nucleus can receive an atom from the a matrix. This will depend on the surface area of the nucleus and the rate at which diffusion can occur. If the activation energy for atomic migration is ΔG_m per atom, f can be written as ω exp $(-\Delta G_m/kT)$ where ω is a factor that includes the vibration frequency of the atoms and the area of the critical nucleus. The nucleation rate will therefore be of the form

$$N_{\text{hom}} = \omega C_0 \exp\left(-\frac{\Delta G_m}{\text{kT}}\right)\exp\left(-\frac{\Delta G^*}{kT}\right)$$

In order to evaluate this equation as a function of temperature ω and ΔG_m can be assumed to be constant, but ΔG^* will be strongly temperature dependent. The main factor controlling ΔG^* is the driving force for precipitation ΔG_V. Since composition is variable the magnitude of ΔG_V must be obtained from the free energy– composition diagram.

If the alloy X_0 in Fig, is solution treated at T_1 and then cooled rapidly to T_2 it will become supersaturated with B and will try to precipitate β.

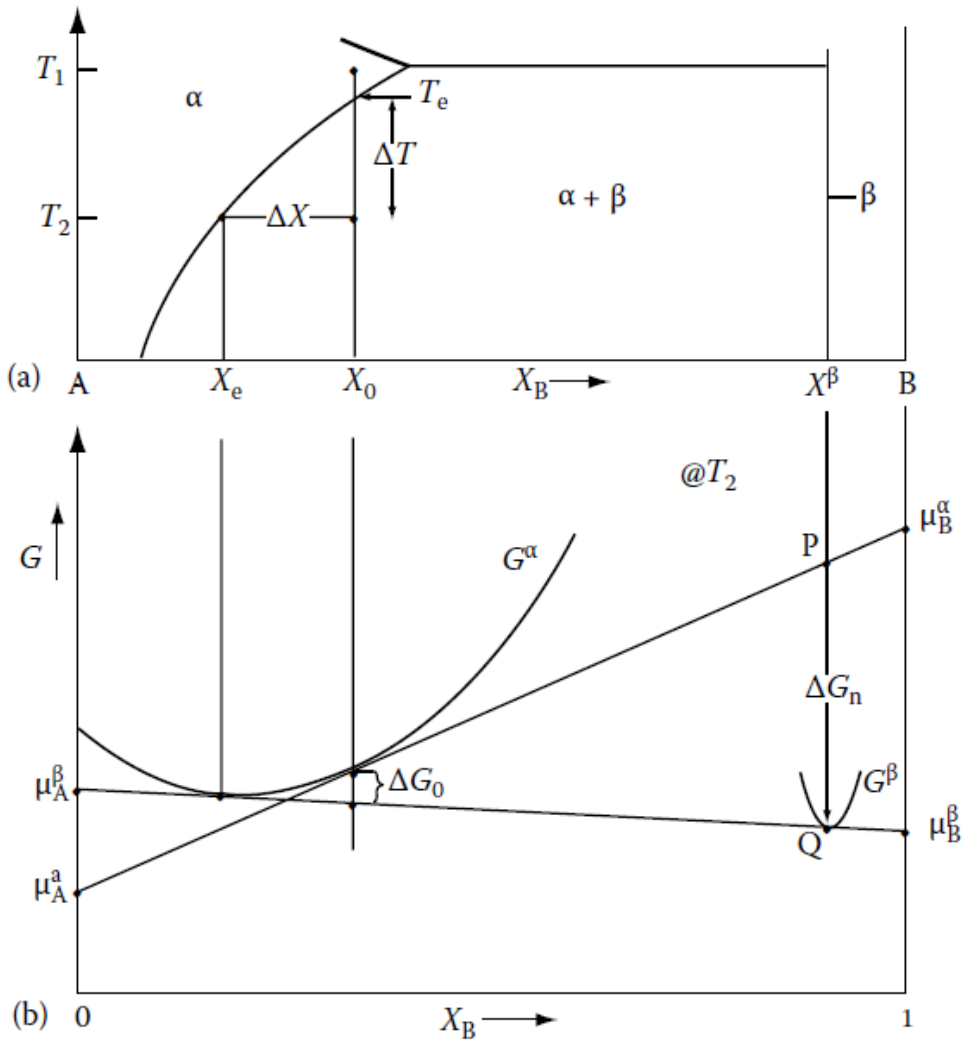

Free energy changes during precipitation. The driving force for the first precipitates to nucleate is $\Delta G_n = \Delta G_v V_m$ ΔG_0 is the total decrease in free energy when precipitation is complete and equilibrium has been reached.

When the transformation to $\alpha + \beta$ is complete the free energy of the alloy will have decreased by an amount ΔG_0 per mole as shown in Fig-b. ΔG_0 is therefore the total driving force for the transformation. However, it is not the driving force for *nucleation.* This is because the first nuclei to appear do not significantly change the α composition from X_0. The free energy released per mole of nuclei formed can be obtained as follows.

If a small amount of material with the nucleus composition (X_B) β is removed from the α phase, the total free energy of the system will *decrease* by ΔG_1 where

$$\Delta G_1 = \mu_A^\alpha X_A^\beta + \mu_B^\alpha X_B^\beta \qquad \text{(per mol } \beta \text{ remved)}$$

ΔG_1 is a quantity represented by point P in Fig-b. If these atoms are now rearranged into the β crystal structure and replaced, the total free energy of the system will *increase* by an amount

$$\Delta G_2 = \mu_A^\beta X_A^\beta + \mu_B^\beta X_B^\beta \qquad \text{(per mol } \beta \text{ formed)}$$

which is given by point Q. Therefore the driving force for nucleation

$$\Delta G_n = \Delta G_2 - \Delta G_1 \text{ per mol of } \beta$$

which is just the length PQ in Fig-b. The *volume* free energy decrease associated with the nucleation event is therefore simply given by

$$\Delta G_v = \frac{\Delta G_n}{V_m} \text{ per unit volume of } \beta$$

where V_m is the molar volume of β. For dilute solutions it can be shown that approximately

$$\Delta G_v \propto \Delta X \qquad \text{where} \qquad \Delta X = X_0 - X_e$$

From Fig-a therefore it can be seen that the driving force for precipitation increases with increasing undercooling (ΔT) below the equilibrium solvus temperature T_e.

It is now possible to evaluate homogeneous rate equation for alloy X_0 as a function of temperature. The variation of ΔG_V with temperature is shown schematically in Fig-b.

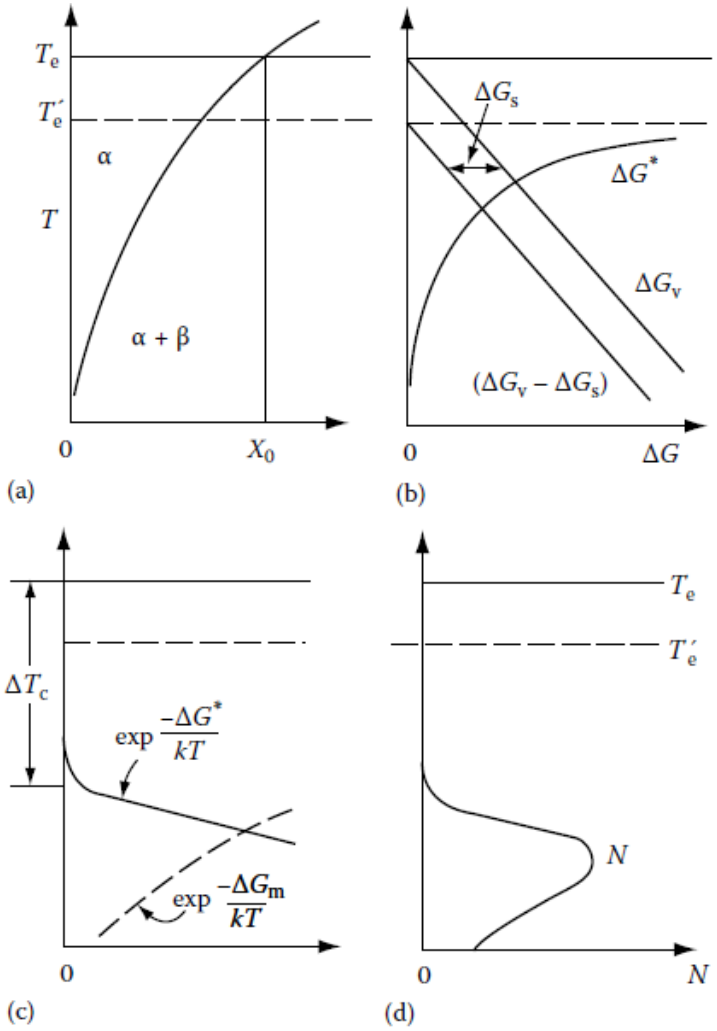

How the rate of homogeneous nucleation varies with undercooling for alloy X_0. (a) The phase diagram, (b) The effective driving force $(\Delta G_V - \Delta G_S)$ and the resultant energy barrier ΔG^*, (c) The two exponential terms that determine N as shown in (d).

After taking into account the misfit strain energy term ΔG_S the effective driving force becomes $(\Delta G_v - \Delta G_s)$ and the effective equilibrium temperature is reduced to T'_e. Knowing $(\Delta G_v - \Delta G_s)$ the activation energy ΔG^* can be calculated. Fig-c shows the two exponential terms in hom. nucleation equation; exp $(-\Delta G^*/kT)$ is essentially the potential concentration of nuclei and, as with nucleation in liquids, this is essentially zero until a critical undercooling ΔT_c is reached, after which it rises very rapidly. The other term, exp $(-\Delta G_m/kT)$, is essentially the atomic mobility. Since ΔG_m is constant this decreases rapidly with decreasing temperature. The combination of these terms, i.e. the homogeneous nucleation rate is shown in Fig-d. Note that at undercoolings smaller than ΔT_c, N is negligible because the driving force ΔG_V is too small, whereas at very high undercoolings N is negligible because diffusion is too slow. A maximum nucleation rate is obtained at intermediate undercoolings.

For alloys containing less solute the critical supercooling will not be reached until lower absolute temperatures where diffusion is slower. The resultant variation of N with T in these alloys will therefore appear as shown in Fig.

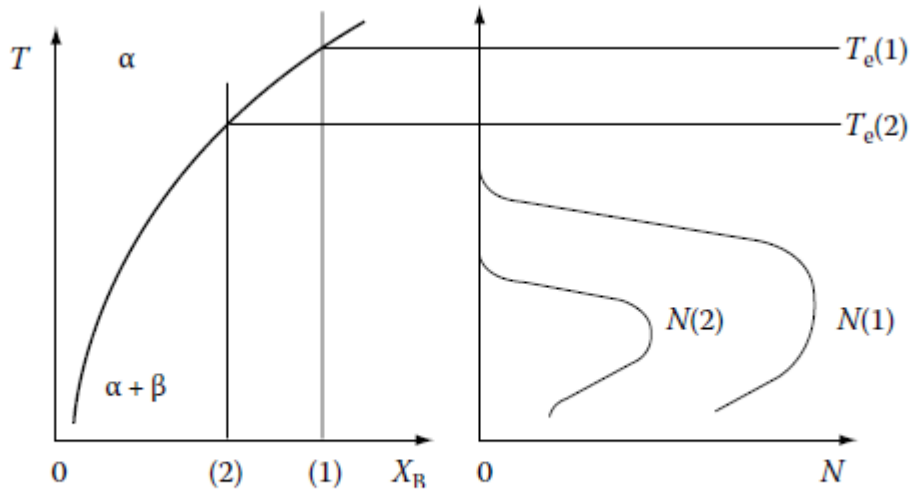

The effect of alloy composition on the nucleation rate. The nucleation rate in alloy 2 is always less than in alloy 1.

In the above treatment of nucleation it has been assumed that the nucleation rate is constant. In practice however the nucleation rate will initially be low, then gradually rise, and finally decrease again as the first nuclei to form start growing and thereby reduce the supersaturation of the remaining α.

It has also been assumed that the nuclei are spherical with the equilibrium composition and structure of the β phase. However, in practice nucleation will be dominated by whatever nucleus has the minimum activation energy barrier ΔG^*. The most effective way of minimizing ΔG^* is by the formation of nuclei with the smallest total interfacial energy. In fact this criterion is dominating in nucleation processes. Incoherent nuclei have such a high value of γ that incoherent homogeneous nucleation is virtually impossible. If, however, the nucleus has an *orientation relationship* with the matrix, and coherent interfaces are formed, ΔG^* is greatly reduced and homogeneous nucleation becomes feasible. The formation of a coherent nucleus will of course increase ΔG_s which decreases T'_e. But below T'_e the decrease in γ resulting from coherency can more than compensate for the increase in ΔG_s.

In most systems the α and β phases have such different crystal structures that it is impossible to form coherent low-energy interfaces and homogeneous nucleation of the equilibrium β phase is then impossible. However, it is often possible to form a coherent nucleus of some other, metastable phase (β) which is not present in the equilibrium phase diagram. The most common example of this is the formation of GP zones which will be discussed in more detail later.

There are a few systems in which the equilibrium phase may nucleate homogeneously. For example in the Cu–Co system Cu alloys containing 1–3% Co can be solution treated and quenched to a temperature where Co precipitates. Both Cu and Co are fcc with only a 2% difference in lattice parameter. Therefore very little coherency strain is associated with the formation of coherent Co particles. The interfacial energy is about 200 mJ m^{-2} and the critical undercooling for measurable homogeneous nucleation is about 40°C.

This system has been used to experimentally test the theories of homogeneous nucleation and reasonably close agreement was found.

Another system in which the equilibrium phase is probably formed homogeneously at a few tens of degrees undercooling is the precipitation of Ni_3Al in many Ni-rich alloys. Depending on the system the misfit varies up to a maximum of 2%, and γ is probably less than 30 mJ m^{-2}. Most other examples of homogeneous nucleation, however, are limited to metastable phases, usually GP zones.

Heterogeneous Nucleation

Nucleation in solids, as in liquids, is almost always heterogeneous. Suitable nucleation sites are non-equilibrium defects such as excess vacancies, dislocations, grain boundaries, stacking faults, inclusions, and free surfaces, all of which increase the free energy of the material. If the creation of a nucleus results in the destruction of a defect, some free energy (ΔG_d) will be released thereby reducing (or even removing) the activation energy barrier. Equation for heterogeneous nucleation is

$$\Delta G_{\text{het}} = -V(\Delta G_v - \Delta G_s) + A\gamma - \Delta G\text{d}$$

Nucleation on Grain Boundaries

Ignoring any misfit strain energy, the optimum embryo shape should be that which minimizes the total interfacial free energy. The optimum shape for an *incoherent* grain-boundary nucleus will consequently be two abutted spherical caps as shown in Fig, with θ given by

$$\cos\theta = \gamma_{\alpha\alpha}/2\gamma_{\alpha\beta}$$

(assuming $\gamma_{\alpha\beta}$ is isotropic and equal for both grains). The excess free energy associated with the embryo will be given by $\Delta G = -V\Delta G_v + A_{\alpha\beta}\gamma_{\alpha\beta} - A_{\alpha\alpha}\gamma_{\alpha\alpha}$

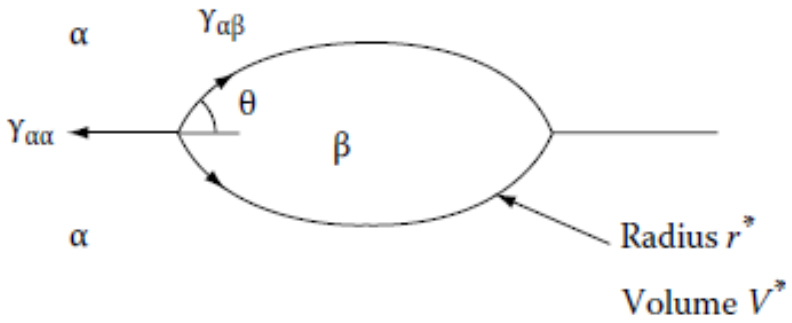

The critical nucleus size (V^*) for grain boundary nucleation.

where V is the volume of the embryo, $A_{\alpha\beta}$ is the area of α/β interface of energy $\gamma_{\alpha\beta}$ created, and $A_{\alpha\alpha}$ the area of α/α grain boundary of energy $\gamma_{\alpha\beta}$ destroyed during the process. The last term of the above equation is simply ΔG_d

It can be seen that grain boundary nucleation is analogous to solidification on a substrate and the same results will apply. Again the critical radius of the spherical caps will be independent of the grain boundary and given by

$$r^* = 2\gamma_{\alpha\beta}/\Delta G_v$$

and the activation energy barrier for heterogeneous nucleation will be given by

$$\frac{\Delta G^*_{\text{het}}}{\Delta G^*_{\text{hom}}} = \frac{V^*_{\text{het}}}{V^*_{\text{hom}}} = S(\theta)$$

where $S(\theta)$ is a shape factor given by $S(\theta) = \frac{1}{2}(2+\cos\theta)(1-\cos\theta)^2$

The ability of a grain boundary to reduce $\Delta G_{\text{het}}{}^*$, i.e. its potency as a nucleation site, depends on cos θ, i.e. on the ratio $\gamma_{\alpha\alpha}/\gamma_{\alpha\beta}$. If this ratio exceeds 2, then there is no nucleation barrier

V^* and ΔG^* can be reduced even further by nucleation on a grain edge or grain corner, Figs. below shows how $\Delta G^*_{\text{het}} / \Delta G^*_{\text{hom}}$ depends on cos θ for the various grain boundary nucleation sites

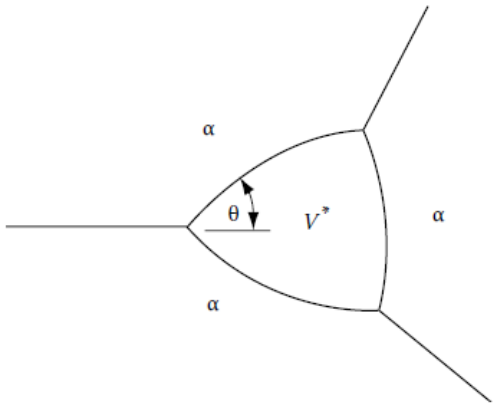

Critical nucleus shape for nucleation on a grain edge.

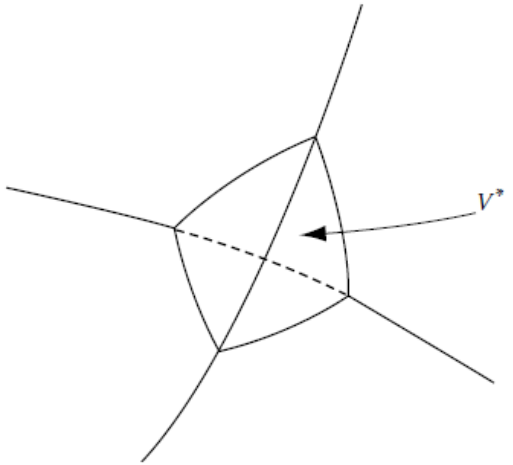

Critical nucleus shape for nucleation on a grain corner.

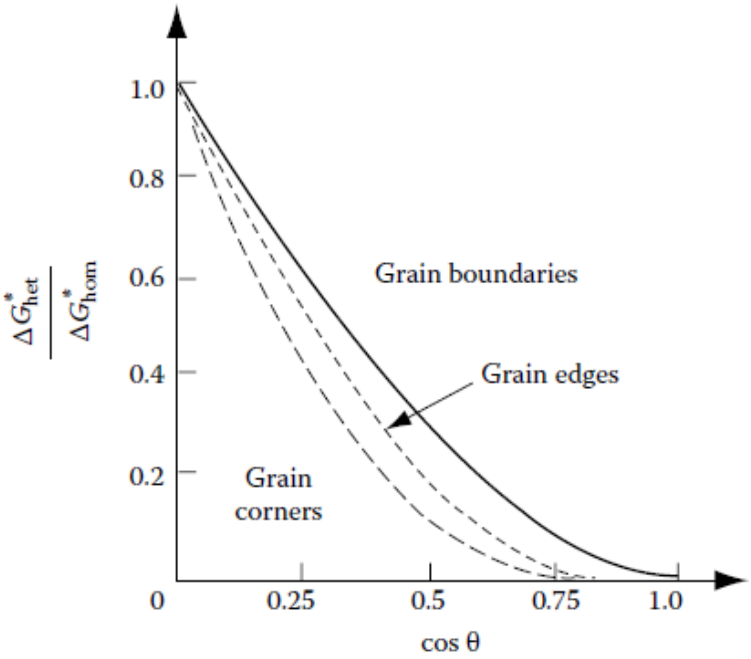

The effect of θ on the activation energy for grain boundary nucleation relative to homogeneous nucleation. (After J.W. Cahn, *Acta Metallurgia* 4 (1956) 449.)

Rate of Heterogeneous Nucleation

If the various nucleation sites are arranged in order of increasing ΔG_d, i.e. decreasing ΔG^*, the sequence would be roughly

1. homogeneous sites
2. vacancies
3. dislocations
4. stacking faults
5. grain boundaries and interphase boundaries
6. free surfaces.

Nucleation should always occur most rapidly on sites near the bottom of the list. However the relative importance of these sites in determining the overall rate at which the alloy will transform also depends on the relative concentrations of the sites.

If the concentration of heterogeneous nucleation sites is C_1 *per unit volume,* the heterogeneous nucleation rate will be given by an equation of the form

$$N_{het} = \omega C_1 \exp\left(-\frac{\Delta G_m}{kT}\right).\exp\left(-\frac{\Delta G^*}{kT}\right) \text{ nuclei m}^{-3}\text{s}^{-1}$$

The relative magnitudes of the heterogeneous and homogeneous volume nucleation rates can be obtained by dividing relative equations giving

$$\frac{N_{het}}{N_{hom}} = \frac{C_1}{C_0}\exp\left(\frac{\Delta G^*_{hom} - \Delta G^*_{het}}{kT}\right)$$

(Differences in ω and ΔG_m are not so important and have been ignored.)

Since ΔG^* is always smallest for heterogeneous nucleation the exponential factor in the above equation is always a large quantity which favours a high heterogeneous nucleation rate. However, the factor (C_1/C_0) must also be taken into account, i.e. the number of atoms on heterogeneous sites relative to the number within the matrix.

For grain boundary nucleation $$\frac{C_1}{C_0} = \frac{\delta}{D}$$

where δ is the boundary thickness and D is the grain size.

Overall Transformation Kinetics—TTT Diagrams

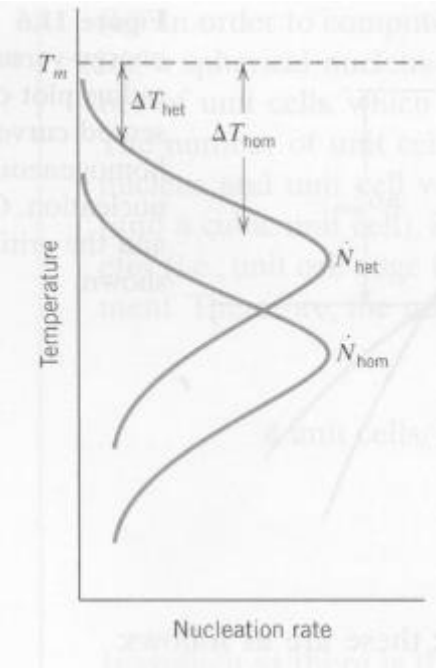

Particle growth occurs by long-range atomic diffusion, which normally involves several steps- for example, diffusion through the parent phase, across a phase boundary, and then into the nucleus. Consequently, the growth rate $\dot{G}$ is determined by the rate of diffusion, and its temperature dependence is the same for the diffusion coefficient.

$$\dot{G} = C\exp\left(-\frac{Q}{kT}\right)$$

where Q is the activation energy and C is preexponential and independent of temperature. The temperature dependence of $\dot{G}$ is represented by

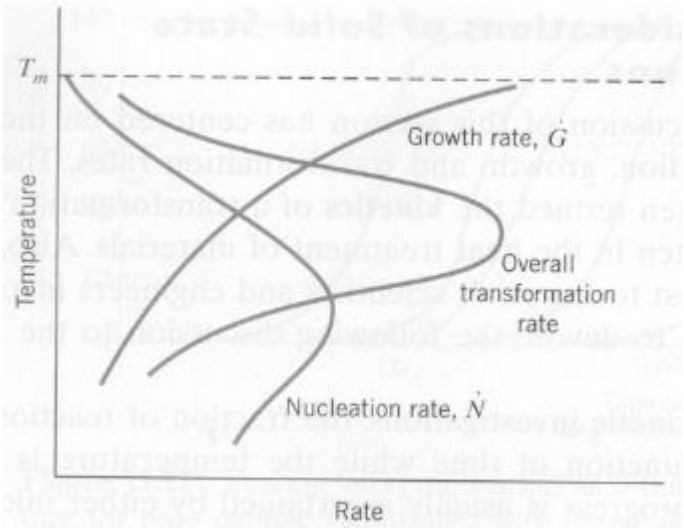

Also shown is a curve for heterogeneous nucleation rate. The overall transformation rate is equal to sum of $\dot{G}$ and $\dot{N}$. The general shape of this curve is the same as for the nucleation rate, in that it has a peak or maximum that has been shifted upward relative to $\dot{N}$ curve.

The rate of transformation and the time required for the transformation to proceed to some degree of completion (e.g time to 50% reaction completion, $t_{0.5}$) are inversely proportional to one another.

$$\text{rate} = \frac{1}{t_{0.5}}$$

Therefore if the logarithm of this transformation the ($\log t_{0.5}$) is plotted vs temperature, a curve will have a general shape as shown below.

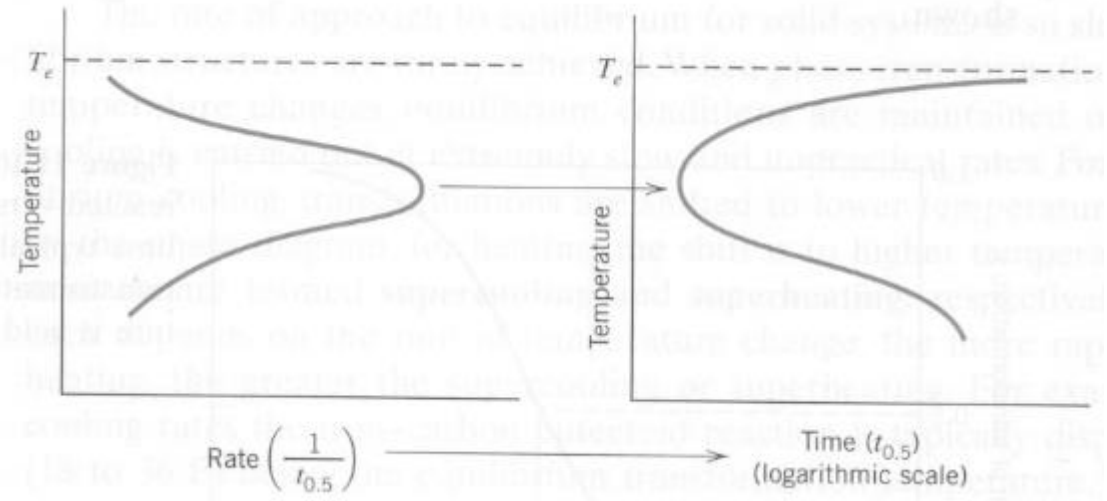

The progress of an isothermal phase transformation can be conveniently represented by plotting the fraction transformation (f) as a function of time and temperature, i.e. a TTT diagram as shown in Fig-a. For transformations of the type $\alpha \rightarrow \beta$, f is just the volume fraction of β at any time. In both cases f varies from 0 to 1 from the beginning to the end of the transformation, Fig-b.

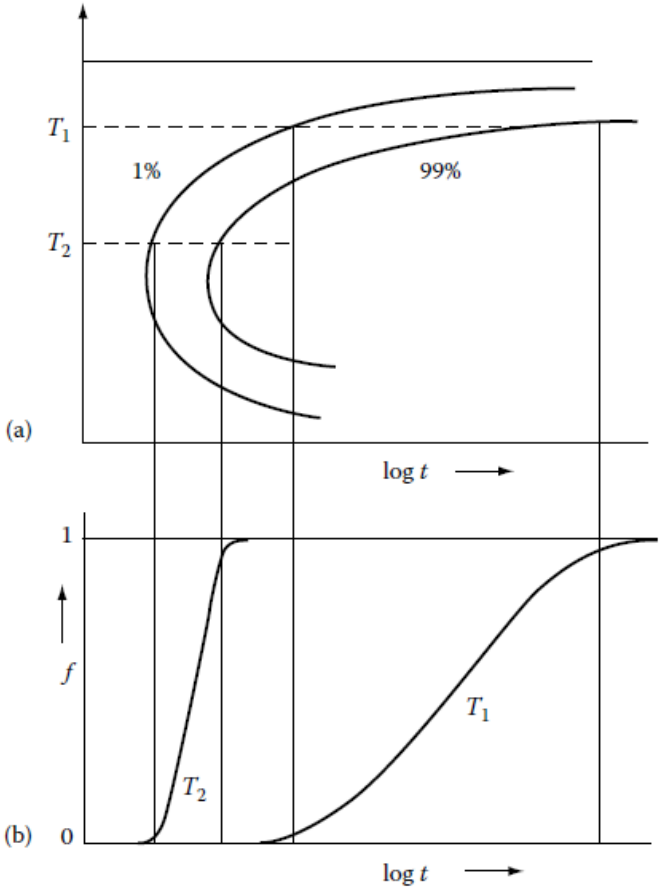

The percentage transformation versus time for different transformation temperatures.

Among the factors that determine $f(t, T)$ are the nucleation rate, the growth rate, the density and distribution of nucleation sites, the overlap of diffusion fields from adjacent transformed volumes, and the impingement of adjacent transformed volumes. Some of the problems involved are illustrated in Fig.

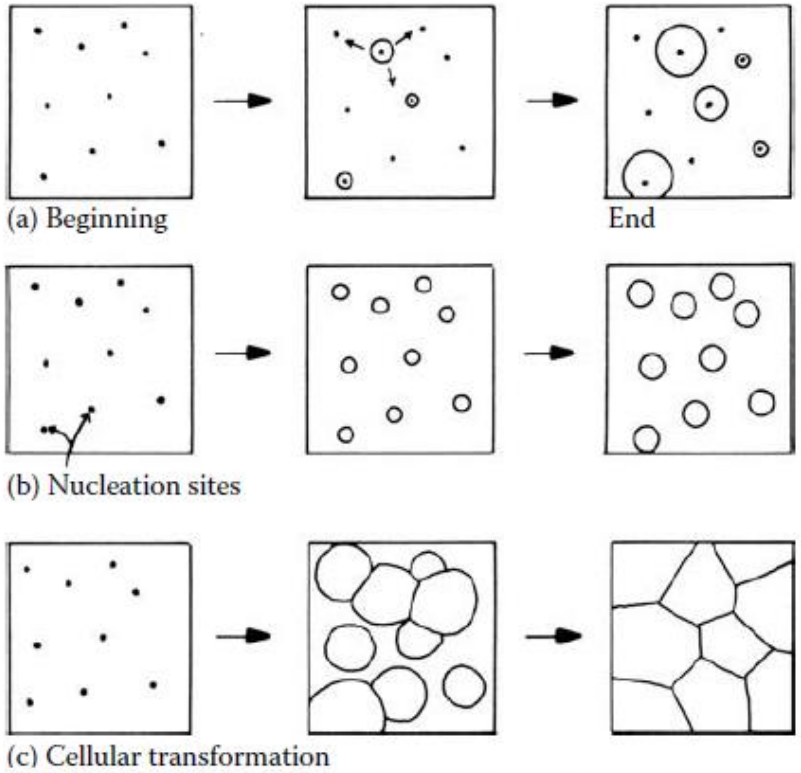

(a) Nucleation at a constant rate during the whole transformation, (b) Site saturation—all nucleation occurs at the beginning of transformation, (c) A cellular transformation.

After quenching to the transformation temperature the metastable a phase will contain many nucleation sites (usually heterogeneous). One possible sequences of events, Fig-a, is that nuclei form throughout the transformation so that a wide range of particle sizes exists at any time. Another possibility is that all nuclei form right at the beginning of transformation, Fig-b. If all potential nucleation sites are consumed in the process this is known as *site saturation.* In Fig-a, *f* will depend on the nucleation rate and the growth rate. In Fig-b, *f* will only depend on the number of nucleation sites and the growth rate. For transformations of the type $\alpha \rightarrow \beta$ or $\alpha \rightarrow \beta + \gamma$ (known collectively as *cellular transformations*) all of the parent phase is consumed by the transformation product, Fig-c. In these cases the transformation does not terminate by the gradual reduction in the growth rate, but by the impingement of adjacent cells growing with a constant velocity. Pearlite, cellular precipitation, massive transformations and recrystallization belong to this category.

Civilian transformations that occur on cooling are typified by C-shaped TTT curves as shown before Fig-a. This can be explained on the basis of the variation of nucleation and growth rates with increasing undercooling. At temperatures close to T_e the driving force for transformation is very small although growth rate can be very high, because nucleation rates are very slow and a long time is required for transformation. When ΔT is very large, on the other hand, slow diffusion rates limit the rate of transformation. A maximum rate is, therefore, obtained at intermediate temperatures.

Precipitation in Aluminum-Copper Alloys

GP Zones

Fig shows the Al–rich end of the Al–Cu phase diagram. If an alloy with the composition Al–4 wt% Cu is heated to a temperature of about 540°C all copper will be in solid solution as a stable fcc α phase, andby quenching the specimen rapidly into water there is no time for any transformation to occur so that the

solid solution is retained largely unchanged to room temperature, However, the solid solution is now supersaturated with Cu and there is a driving force for precipitation of the equilibrium θ phase, $CuAl_2$.

.

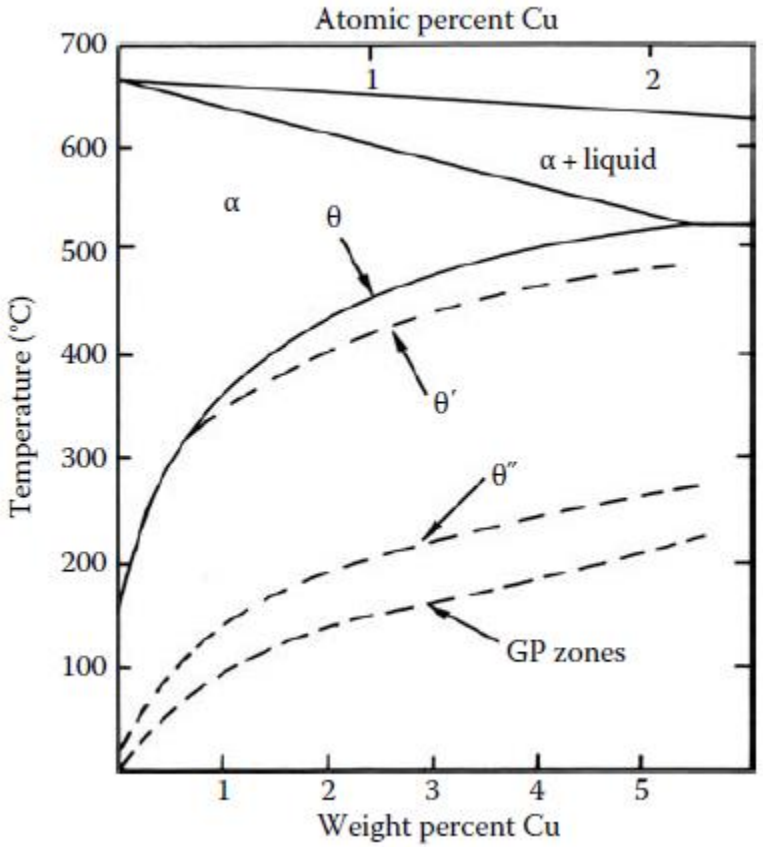

If the alloy is now *aged* by holding for a period of time at room temperature or some other temperature below about 180°C it is found that the first precipitate to nucleate is not θ but coherent Cu-rich GP zones. (Copper-rich zones in Al–Cu alloys were detected independently in 1938 by Guinier and Preston from streaks in X-ray diffraction patterns.) The reason for this can be understood on the basis of the relative activation energy barriers for nucleation as discussed earlier. GP zones are fully coherent with the matrix and therefore have a very low interfacial energy, whereas the θ phase has a complex tetragonal crystal structure which can only form with high-energy incoherent interfaces. In addition, the zones minimize their strain energy by choosing a disc-shape perpendicular to the elastically soft ⟨100⟩ directions in the fcc matrix. Therefore, despite the fact that the driving force for precipitation of GP zones ($\Delta G_V - \Delta G_S$) is less than for the equilibrium phase, the barrier to nucleation (ΔG^*) is still less, and the zones nucleate most rapidly.

GP zones are formed as the first precipitate during low-temperature ageing of many technologically important alloys, notably those based on aluminum (see Table). In dilute Al–Zn and Al–Ag alloys Zn–rich and Ag-rich GP zones are found. In these cases there is very little misfit strain and ΔG^* is minimized by the formation of spherical zones with a minimum interfacial energy.

Some Precipitation-Hardening Sequences

Base Metal	Alloy	Precipitation Sequence
Aluminum	Al–Ag	GPZ (spheres) → γ'(plates) → $\gamma(Ag_2Al)$
	Al–Cu	GPZ (discs) → θ'(discs) → θ'(plates) → $\theta(CuAl_2)$
	Al–Cu-Mg	GPZ (rods) → S' (laths) → $S(CuMgAl_2)$ (laths)
	Al–Zn–Mg	GPZ(spheres) → η'(plates) → $\eta(MgZn_2)$
	Al–Mg–Si	GPZ (rods) → β' (rods) → $\beta(Mg_2Si)$ (plates)
Copper	Cu–Be	GPZ (discs) → γ(CuBe)
	Cu–Co	GPZ (spheres) → β(Co) (plates)
Iron	Fe–C	ε-carbide (discs) → Fe_3C(plates)
	Fe–N	α'(discs) → Fe_4N
Nickel	Ni–Cr–Ti–Al	γ'(cubes or spheres)

Source: Mainly from J.W. Martin, Precipitation Hardening, Pergamon Press, Oxford, 1968.

Transition Phases

The formation of GP zones is usually followed by the precipitation of so-called transition phases. In the case of Al–Cu alloys the equilibrium θ phase is preceded by θ'' and θ'. The total precipitation process can be written $\alpha_0 \rightarrow \alpha_1$ + GP zones$\rightarrow \alpha_2 + \theta'' \rightarrow \alpha_3 + \theta' \rightarrow \alpha_4 + \theta$ where α_0 is the original supersaturated solid solution, α_1 is the composition of the matrix in equilibrium with GP zones, α_2 the composition in equilibrium with θ'' etc. Fig shows a schematic free energy diagram for the above phases. Since GP zones and the matrix have the same crystal structure they lie on the same free energy curve (ignoring strain energy effects—see Section 5.5.5).

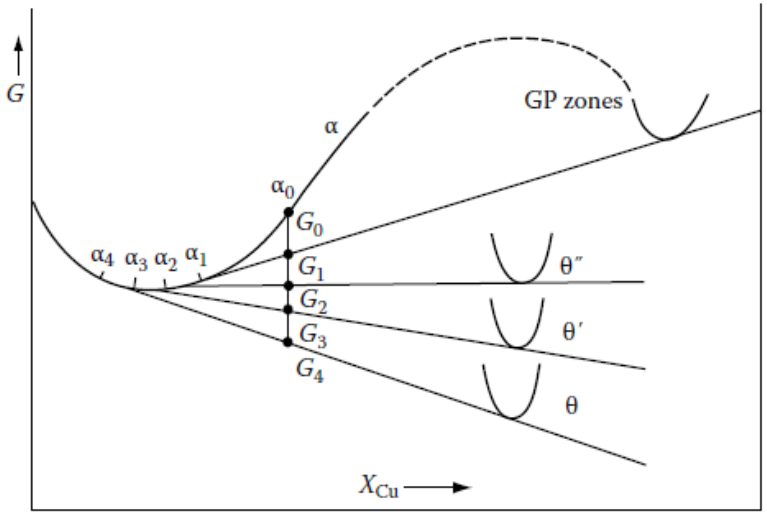

The transition phases θ'' and θ' are less stable than the equilibrium θ phase and consequently have higher free energies as shown. The compositions of the matrix in equilibrium with each phase—$\alpha_1\alpha_2\alpha_3\alpha_4$—are given by the common tangent construction. These compositions correspond to points on the solvus lines for GP zones, θ'', $\theta'$and θ shown in Fig before. The free energy of the alloy undergoing the above precipitation sequence decreases as shown in related fig.

$$G_0 \rightarrow G_1 \rightarrow G_2 \rightarrow G_3 \rightarrow G_4$$

Transformation stops when the minimum free energy equilibrium state $G4$ is reached, i.e. α_4 + θ.

Transition phases form because, like GP zones, they have a lower activation energy barrier for nucleation than the equilibrium phase, Fig-a. The free energy of the alloy therefore decreases more rapidly via the transition phases than by direct transformation to the equilibrium phase, Fig-b.

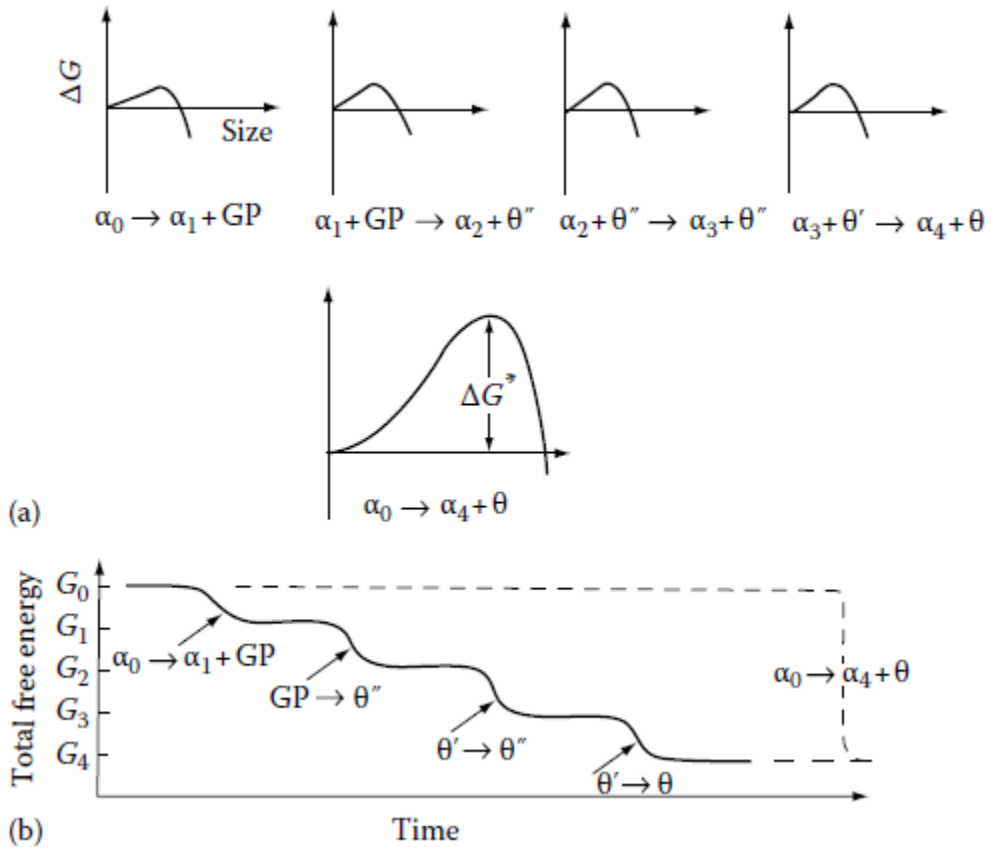

The lower activation energy barriers are achieved because the crystal structures of the transition phases are intermediate between those of the matrix and the equilibrium phase. In this way the transition phases can achieve a high degree of coherence and thus a low interfacial energy contribution to ΔG^*. The equilibrium phase on the other hand usually has a complex crystal structure that is incompatible with the matrix and results in high-energy interfaces and high ΔG^*.

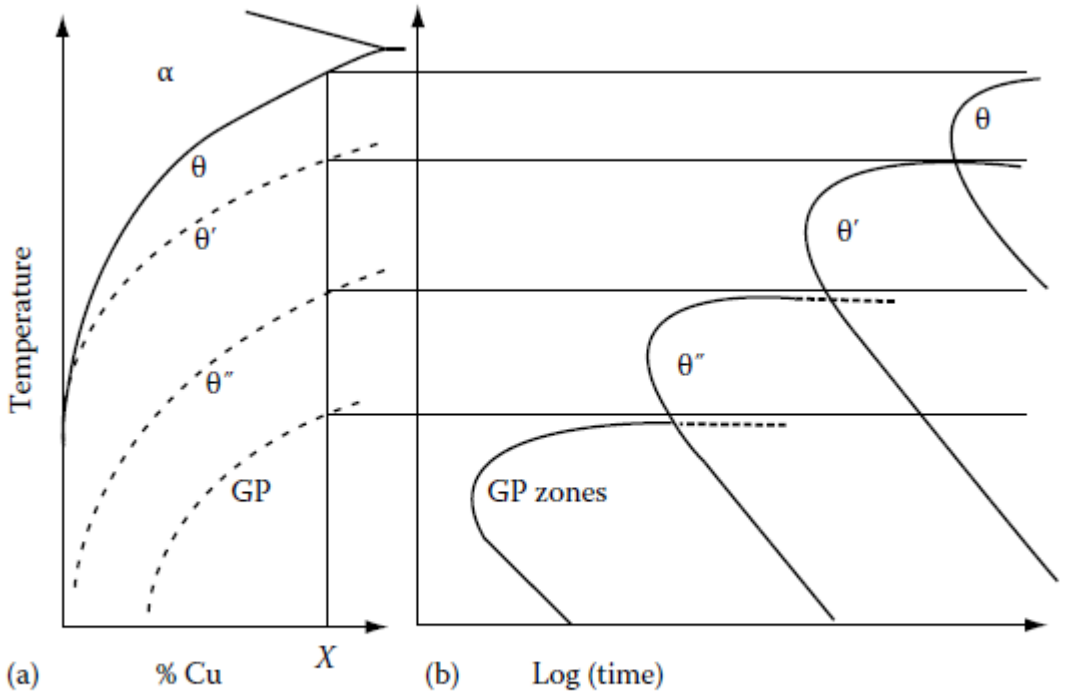

(a) Metastable solvus lines in Al–Cu (schematic), (b) Time for start of precipitation at different temperatures for alloy *X* in (a).

Quenched-in Vacancies

It was shown in the beginning of the course that the equilibrium concentration of vacancies increases exponentially with temperature. Thus the *equilibrium* vacancy concentration will be relatively high at the solution treatment temperature and much lower at the ageing temperature. However, when the alloy is rapidly quenched from the high temperature there will be no time for the new equilibrium concentration to be established and the high vacancy concentration becomes *quenched-in.* Given time, those vacancies in excess of the equilibrium concentration will *anneal out.* There will be a tendency for vacancies to be attracted together into *vacancy clusters,* and some clusters collapse into dislocation loops which can grow by absorbing more vacancies. The dislocations that are already present can also absorb vacancies by *climbing.* In this way straight screw dislocations can become converted into longer helical edge dislocations. There are many ways, therefore, in which excess vacancies are able to provide heterogeneous nucleation sites.

Another effect of quenched-in vacancies is to greatly increase the rate at which atoms can diffuse at the ageing temperatures. This in turn speeds up the process of nucleation and growth. Indeed the only way of explaining the rapid formation of GP zones at the relatively low ageing temperatures used is by the presence of excess vacancies. If GP zones are separated by a mean spacing λ, the mean diffusion distance for the solute atoms is $\lambda/2$. Therefore, if the zones are observed to form in a time t, the effective diffusion coefficient is roughly given by x^2/t, i.e.

$$D \simeq \frac{\lambda^2}{4t}$$

If high-temperature diffusion data are extrapolated down to the ageing temperature, the values obtained are orders of magnitude smaller than the above value. The difference can, however, be explained by a quenched-in vacancy concentration that is orders of magnitude greater than the equilibrium value. In Al-Cu alloys, for example, GP zones can form by ageing at room temperature, which would not be feasible without assistance from excess vacancies.